Asymmetric Metal-Insulator Transition in Disordered Ferromagnetic Films

R. Misra, A. F. Hebard,* and K. A. Muttalib
Department of Physics, University of Florida, Gainesville, Florida 32611-8440, USA

P. Wölfle
Institute for Condensed Matter Theory and Institute for Nanotechnology, Karlsruhe Institute of Technology, D-76128 Karlsruhe, Germany

(Received 22 March 2010; published 11 July 2011)

We present experimental data and a theoretical interpretation of the conductance near the metal-insulator transition in thin ferromagnetic Gd films of thickness $b \approx 2$–10 nm. A large phase relaxation rate caused by scattering of quasiparticles off spin-wave excitations renders the dephasing length $L_\phi \lesssim b$ in the range of sheet resistances considered, so that the effective dimension is $d = 3$. The conductivity data at different stages of disorder obey a fractional power-law temperature dependence and collapse onto two scaling curves for the metallic and insulating regimes, indicating an asymmetric metal-insulator transition with two distinctly different critical exponents; the best fit is obtained for a dynamical exponent $z \approx 2.5$ and a correlation (localization) length critical exponent $\nu_- \approx 1.4$ ($\nu_+ \approx 0.8$) on the metallic (insulating) side.

DOI: 10.1103/PhysRevLett.107.037201 PACS numbers: 75.45.+j, 75.50.Cc, 75.70.Ak

The metal-insulator (*M-I*) transition in disordered conductors [1] has been one of the most extensively studied cases of a quantum phase transition. In its simplest form it describes noninteracting electrons in a disordered potential, where the disorder can be controlled experimentally in a variety of ways, e.g., by systematic doping. One of the most dramatic predictions of the scaling theory [1] is the absence of true metallic behavior in systems with dimension $d \leq 2$ as verified in numerous experiments [2]. The other prediction is the existence of a critical point in $d > 2$ where the conductivity in the metallic phase goes to zero continuously with increasing disorder, in contrast to having a minimum metallic conductivity [3]. Electron-electron interactions are known to modify the behavior near a *M-I* transition in a significant way [4], including the possibility of a metallic state in $d = 2$ [5].

Near the transition, the behavior is characterized by power laws with critical exponents. For example, the dc conductivity $\sigma(\lambda)$, with λ being a measure of disorder, follows a power law $\sigma \sim t^s$, where $t = (1 - \lambda/\lambda_c)$ denotes the distance to the critical point at critical disorder λ_c, and s is the conductivity exponent. The dynamical conductivity at the critical point, on the other hand, is characterized by the dynamical exponent z as $\sigma(\omega; \lambda_c) \sim \omega^{1/z}$. The correlation length on the metallic side ($\lambda < \lambda_c$) diverges at the critical point as $\xi \sim t^{-\nu_-}$ and the localization length ($\lambda > \lambda_c$) diverges as $\xi \sim |t|^{-\nu_+}$. In $d = 3$ dimensions the relation $s = \nu_-$ holds. The exponents in $d = 3$ have yet to be calculated in a reliable way. While the critical exponents ν_+ and ν_- may in principle be different, all theoretical and experimental works so far have either assumed or observed $\nu_+ = \nu_-$. In contrast, we report here that for ferromagnetic thin films the two exponents are distinctly different, describing a very unusual asymmetric transition.

Critical exponents cannot be measured experimentally at the $T = 0$ critical point but must be inferred from finite T measurements. Therefore, the emphasis has been to obtain the conductivity as a function of T, as close to $T = 0$ as possible. Despite intense efforts over several decades [6], it turned out to be rather difficult to access the critical regime in a reliable way. While all such experiments confirm the continuous nature of the transition, the values of the critical exponents remain controversial. Experimental values of s and z vary from $s \approx 0.5$ [7], $s \approx 1$ [8,9] to $s \approx 1.6$ and from $z \approx 2$ [10] to $z \approx 2.94$ [11]. For the Anderson localization transition (omitting interaction effects), numerical studies find $s \approx 1.6$ [12] while theoretical studies find $z = 3$ [13].

Theoretically, the scale dependent conductivity at finite T is obtained from $\sigma(\omega)$ by replacing ω by T. The critical dynamical scaling is found even away from the critical point in the regime defined by frequencies $\omega \geq \omega_\xi = \frac{1}{\tau}(\xi/l)^{-z}$. Here l and τ are the mean free path and the momentum relaxation time, respectively. Near the quantum critical point, $\sigma(\omega)$ obeys the scaling law,

$$\sigma(\omega; \lambda) = \xi^{-1} G(\pm 1, \xi\omega^{1/z}), \qquad t \gtrless 0. \tag{1}$$

At the critical point, when $\xi \to \infty$, it follows that $G(\pm 1, \xi\omega^{1/z}) \sim \xi\omega^{1/z}$. Using the sheet resistance R_0 as the disorder parameter controlled in experiment and R_c denoting the critical resistance so that $\xi \propto |R_0 - R_c|^{-\nu_\pm}$ where $\nu_\pm$ is either ν_+ or ν_- depending on whether R_0 is larger or smaller than R_c, and replacing ω by T, the conductivity should obey the scaling law,

$$|\epsilon|^{-\nu_\pm}\sigma(T;R_0) = G(\pm 1, |\epsilon|^{-\nu_\pm}T^{1/z}), \quad \epsilon \equiv R_0 - R_c. \qquad (2)$$

Below we will see that for thin ferromagnetic Gd films, the exponent $\nu_\pm$ is distinctly different on the two sides of the transition, i.e., $\nu_+ \neq \nu_-$. Such measurements on ferromagnetic films have not been carried out in the past because samples are highly air sensitive; we use a specialized apparatus in which the sample can be transferred without exposure to air from the high vacuum deposition chamber to an adjoining low-temperature cryostat and electrically reconnected for transport measurements.

We study the conductivity near the *M-I* transition in a thin-film geometry where disorder is controlled by varying the film deposition rate, the thickness, and by annealing [14]. The resulting sheet resistance is the single important parameter controlling the distance to the critical point. Two series of thin films of Gd (series 1 and series 2) were grown by rf magnetron sputtering through a shadow mask onto sapphire substrates held at $T = 130$ K. The electrical leads of the deposited sample overlapped with predeposited palladium contacts, thus allowing reliable low contact resistance connection for *in situ* measurements of the electrical properties. Immediately after deposition the samples were transferred to the cryostat and held at $T = 77$ K or below where the samples are stable. If the temperature is temporarily raised back to the deposition temperature (130 K), annealing marked by a slow irreversible increase in resistance occurs.

The amount of disorder in a given film is parametrized by the longitudinal sheet resistance $R_0 \equiv R_{xx}(T = 5\ \mathrm{K})$ [15,16]. In our experiments R_0 spans the range $4 < R_0 < 70\ \mathrm{k\Omega}$, which for most of the samples guarantees that the conductivity at all temperatures is mostly determined by strongly localized quantum wave packets. For thicker films at lower disorder strength ($450 < R_0 < 2840\ \Omega$), quantum corrections due to weak localization and spin-wave mediated electron-electron interactions have been observed and interpreted [16].

Controlled thermal annealing allows us to advantageously tune a single sample through successive stages of increased disorder. Our series 1 samples comprise 5 separate depositions with two of the samples undergoing 12 successive anneals thus giving a total of 17 measurements. Our series 2 samples comprise a single sample undergoing 15 successive anneals for a total of 16 measurements spanning the critical region. The resistance was measured using four-terminal dc techniques, and excellent reproducibility between all samples was found.

Our films are effectively three dimensional since the phase relaxation rate τ_φ in ferromagnetic films is dominated by the scattering off spin-wave excitations [16]. For a spin-wave gap $\Delta \ll \hbar/\tau_\varphi$ as observed in Gd [17], the rate is given by [18] $\hbar/\tau_\varphi = [\frac{nJ^2}{\pi^2\hbar}\frac{D}{D^2+(A/\hbar)^2}\frac{T}{\sqrt{A}}]^{2/3}$ in $d = 3$. Here n is the electron density, $\bar{J} \approx nJ \approx 80$ meV is the exchange energy [19], and $A \approx \bar{J}/k_F^2$ is the spin-wave stiffness. The T-dependent diffusion coefficient D may be obtained from the resistivity by $D = 1/(Rbe^2N_0)$, where N_0 is the 3D density of states and b is the film thickness. The dimensionality of the system is $d = 3$ if the T-dependent dephasing length [2] $L_\varphi(T) = \sqrt{D\tau_\varphi} \ll b$. Near the critical point, we use $R(T) = R_0(T_0/T)^p$, where $T_0 = 5$ K, and $R_0 \approx 1/L_0 = 25.81\ \mathrm{k\Omega}$, where $L_0 = e^2/h$. Using $b = 2$ nm and estimates for Fermi wave vector k_F and N_0 from Ref. [19], we obtain $L_\varphi \approx 1(T/T_0)^{(5p-2)/6}$ nm. We will see later that experimentally $p \approx 0.4$, which makes L_φ essentially T independent. Three dimensionality is assured since L_ϕ of a disordered ferromagnetic system is much shorter than that of a nonmagnetic system.

In Fig. 1 we show raw data for longitudinal conductivity σ_{xx} (normalized by L_0) as a function of T, for all our samples characterized by their sheet resistance R_0 in the range $15 < R_0 < 31\ \mathrm{k\Omega}$. Within this range (fifteen samples), all data can be fit by an expression of the form

$$\sigma(T;R_0)/L_0 = A + BT^p. \qquad (3)$$

The typical high precision of the fits is also shown in Fig. 1 for the sample (solid circles, red fitting line) with fitting values $A = -0.01(1)$, $B = 0.622(9)$, and $p = 0.390(5)$. We emphasize that for all the curves shown, Eq. (3) remains a very good fit with p around 0.4 and relative residual deviations for all data points within the range ± 0.01. Equation (3) is not a statement of scaling but is rather a heuristic ansatz categorizing the data.

Since Eq. (3) is a very good fit for all samples, we can use the three fitting parameters for each sample set to directly calculate reduced activation energy $W(T)$ plots [9] for all 15 samples as is done in Fig. 2, where $W(T) \equiv T[d\ln\sigma(T)/dT] = pBT^p/(A + BT^p)$. We note that since $W \sim p(1 - A/BT^p)$ for $A \ll BT^p$, the plots clearly show

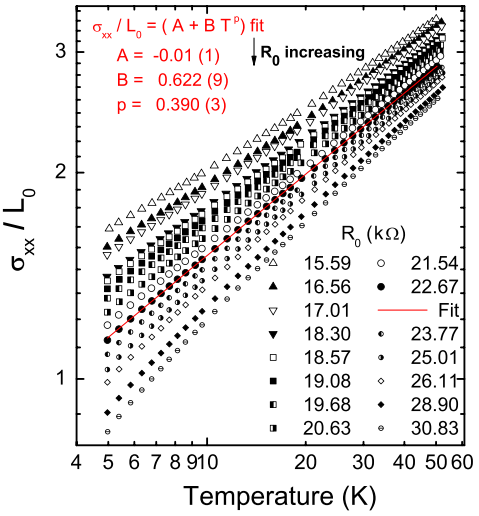

FIG. 1 (color online). Normalized conductivity as a function of temperature in a log-log plot for all samples in the range $15 < R_0 < 31\ \mathrm{k\Omega}$. Fitting of Eq. (3) to one sample (red line) is shown with fitting parameters displayed in the inset.

one flat (T-independent, $A = 0$) separatrix that separates samples which tend to a metallic limit ($dW/dT > 0$, $A > 0$) from samples which tend to an insulating limit ($dW/dT < 0$, $A < 0$). We identify the separatrix as the sample fitted in Fig. 1, with $A = -0.01(1)$. Thus this particular sample happens to be close enough to criticality (pure power law) so that we can confidently make the identification $R_c = 22.67\ \mathrm{k}\Omega$ (which is of order unity in units of h/e^2). As a bonus, using the scaling law, we can also immediately infer from the fitting value of the critical sample, $p = 0.390(5)$, a critical dynamical exponent $z = 1/p \approx 2.5$. Having a sample almost exactly at the critical point allows us to obtain both the critical disorder R_c and the dynamical exponent $z = 1/p$ directly and unambiguously without the need for interpolation.

Our determination of $p = 0.390(5)$ and $R_c = 22.67\ \mathrm{k}\Omega$ at criticality with unprecedented precision allows us to analyze the data in an unbiased way by using a scaling plot of the scaling function G defined in Eq. (2) without using Eq. (3) at all. We take different values of the critical exponents ν_+ and ν_- to see how well the data points collapse onto single curves on both sides of the transition. The best data collapse is found for $\nu_- = 1.38$ ($\nu_+ = 0.77$) on the metallic (insulating) side. The two panels of Fig. 3 show how well the temperature-dependent data for each of the samples indicated in the legends collapse onto linear scaling curves for the two best-fit values of ν_+ and ν_-. We have normalized the axes of each panel to unity using the highest T value of the conductivity of the samples $R_0 = 21.54\ \mathrm{k}\Omega$ ($R_0 = 23.77\ \mathrm{k}\Omega$) closest to criticality on the metallic (insulating) side of the transition.

In the insets to the two panels of Fig. 3, we show the dependence of chi-square (χ^2) on ν_- (ν_+) in the metallic (insulating) regime. The χ^2 calculation is performed using statistical weights proportional to the inverse of the ordinate values, thereby increasing the sensitivity of χ^2 to the data sets close to the origin and hence further away from criticality. The minima of χ^2 are clearly defined for $p = 0.390(5)$ at $\nu_- = 1.38(11)$ [$\nu_+ = 0.77(11)$] in the metallic [insulating] regime. Accordingly, the conductivity exponent s in 3D has been experimentally determined to have the value $s = \nu_- = 1.38(11)$.

It is remarkable that the scaling functions are very well described by straight lines in the regime considered. Thus the conductivity on the metallic side in the temperature regime considered can be represented by an expression reminiscent of Eq. (3) with, however, fixed coefficients B, $p = 1/z$, $\sigma(T; R_0)/L_0 = BT^{1/z} + D_\pm|\epsilon|^{\nu_\pm}$, and disorder independent coefficients $D_\pm$ determined from the intercepts of the linear fits in Fig. 3. More generally, $\sigma(T; R_0)$ and its derivatives are continuous functions of R_0 across the transition point at any finite temperature. This means that, writing the scaling law Eq. (2) as $\sigma(T; R_0)/L_0 = T^{1/z}[B + \tilde{G}_\pm(|\epsilon|^{-\nu_\pm}T^{1/z})]$, all derivatives of $\tilde{G}_\pm(y)$ should vanish in the limit $y \to \infty$; i.e., $\tilde{G}_\pm(y)$ must have an essential singularity at $y \to \infty$. A possible form consistent with the data would be $\tilde{G}_\pm(y) = (D_\pm/y)\exp(-ay)$, where a is a constant. Given that, we conclude that all our data are in the regime $ay \ll 1$.

As pointed out in Ref. [6], reasons for the earlier experiments not agreeing with one another have been traced to difficulties in having a system allowing sufficient access into the critical region and possessing a well-defined

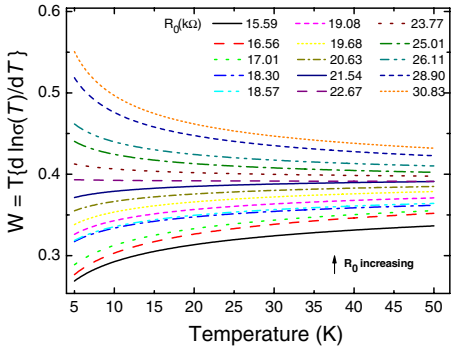

FIG. 2 (color online). W as a function of T, showing the existence of a critical separatrix ($A = 0$) with $R_0 = 22.67\ \mathrm{k}\Omega$, separating the metallic ($A > 0$) and the insulating ($A < 0$) samples.

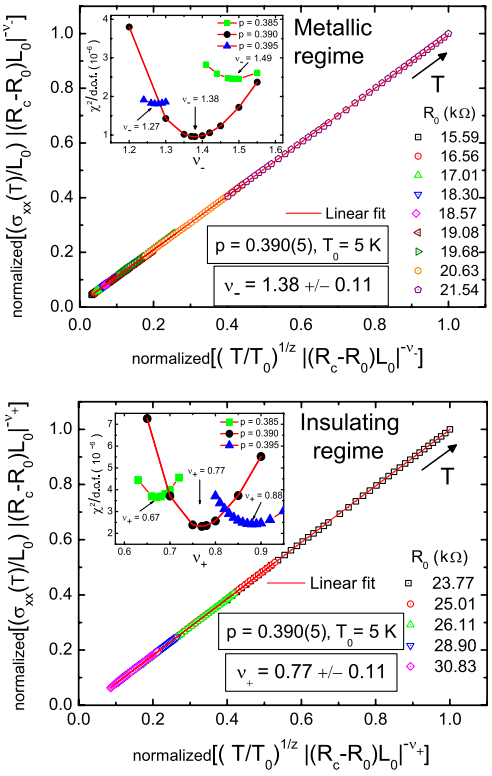

FIG. 3 (color online). Collapse of the data for different values of R_0 according to the scaling relation given by Eq. (2) for $\nu_- = 1.38$ on the metallic side (top panel) and $\nu_+ = 0.77$ on the insulating side (bottom panel). Here $T_0 = 5$ K is a reference temperature. The insets of each panel show the dependence of χ^2 on ν_- and ν_+ for the values of $p = 1/z$ listed in the legends. The best-fit values occur at $p = 0.390(5)$ with well-defined minima at $\nu_- = 1.38(11)$ and $\nu_+ = 0.77(11)$.

critical point. In contrast, the current work is done on a system where the critical point can be clearly identified, and the critical region is experimentally accessible. Note that the number of data sets (14 total) around R_c to be kept in the scaling analysis of Fig. 3 were determined by comparing the χ^2 fits for different number of data points kept. A minimum in χ^2 was obtained for data points restricted to the range 15–31 kΩ. We can also estimate the width of the critical region from the boundary frequency, $\omega_\xi = \frac{1}{\tau}(\xi/l)^{-z} \sim \frac{1}{\tau}(|R_0 - R_c|/R_c)^{\tilde{z}}$, where $\tilde{z}$ is equal to $\nu_- z$ ($\nu_+ z$) on the metallic (insulating) side. At $T \sim 20$ K and using $1/\tau \sim 10^3$ K, this gives $|R_0 - R_c|/R_c \sim 0.4$ (~ 0.2) on the metallic (insulating) side, corresponding to a critical region in the range 15–28 kΩ. This is a sufficiently large experimentally accessible region that allows us to reliably obtain the critical exponents.

Our finding of the two distinctly different values for the critical exponents ν_- and ν_+ in the metallic and insulating phase, respectively, is unexpected [20]. The quality of the data and of the fit to the scaling function shows that the difference of ν_+ and ν_- cannot be explained by uncertainties in the measurement or deviations from the scaling form. Different critical exponents of the correlation length on both sides of the transition may indicate a different structure of critical modes, signaling that the critical dynamics is different on both sides of the transition. In our scaling analysis we assumed one parameter scaling on both sides of the transition, which then leads to different values of the critical exponent ν. A conceivable alternative interpretation is that the scaling changes character, say, on the localized side, such that $\sigma \sim \xi^{-r}$, with $r \sim 0.77/1.38 \sim 1/2$, and $\nu_- = \nu_+$. In other words, one could use either the same length scale on both sides of the transition with different exponents or different scales on the two sides with the same exponent. A change in scaling may be related to charge screening properties that are essentially different in a metal (finite screening length) and in an insulator (infinite screening length). In the ferromagnetic state the screening properties may be modified as well.

To summarize, we have studied the metal-insulator transition in thin ferromagnetic disordered films in an effectively three-dimensional regime experimentally and theoretically. We concentrate on the critical regime, for which the dynamical scaling behavior at the critical point is known to be $\sigma(\omega) \propto \omega^{1/z}$. At finite T the relevant frequencies ω are given by T. A sample with pure power-law dependence $\sigma(T) \propto T^p$ allows us to determine directly and unambiguously the critical resistance $R_c = 22.67$ kΩ as well as the dynamical exponent $z \equiv 1/p \approx 2.5$. A full scaling analysis of the data from a reasonably accessible regime around the critical point ($\pm 30\%$) allows us to determine the critical exponent of the correlation length as $\nu_- = 1.38(11)$ on the metallic side and the localization length exponent $\nu_+ = 0.77(11)$ on the insulating side. This requires the scaling function to have an essential singularity at $R_0 = R_c$ even at finite temperature. The two distinctly different exponents indicate a highly unusual asymmetric quantum phase transition.

We acknowledge discussions with E. Abrahams, R. DeSerio, F. Evers, A. Finkel'stein, Y. Imry, D. Khmelnitskii, and A. Möbius. This work has been supported by the NSF under Grant No. 0704240 (A. F. H.), and by the DFG-Center for Functional Nanostructures (K. A. M., P. W.).

*Corresponding author.
afh@phys.ufl.edu

[1] E. Abrahams *et al.*, Phys. Rev. Lett. **42**, 673 (1979).
[2] See, e.g., P. A. Lee and T. V. Ramakrishnan, Rev. Mod. Phys. **57**, 287 (1985).
[3] N. F. Mott, in *Electronics and Structural Properties of Amorphous Semiconductors*, edited by P. G. Le Comber and J. Mort (Academic, London, 1973).
[4] See, e.g., A. M. Finkel'stein, in *Anderson Localization*, edited by T. Ando and H. Fukuyama (Springer, New York, 1988); D. Belitz and T. R. Kirkpatrick, Rev. Mod. Phys. **66**, 261 (1994).
[5] S. V. Kravchenko and M. P. Sarachik, Rep. Prog. Phys. **67**, 1 (2004); A. Punnoose and A. M. Finkelstein, Science **310**, 289 (2005).
[6] H. Stupp *et al.*, Phys. Rev. Lett. **71**, 2634 (1993); **72**, 2122 (1994).
[7] M. A. Paalanen *et al.*, Phys. Rev. Lett. **48**, 1284 (1982); T. F. Rosenbaum, G. A. Thomas, and M. A. Paalanen, Phys. Rev. Lett. **72**, 2121 (1994).
[8] S. B. Field and T. F. Rosenbaum, Phys. Rev. Lett. **55**, 522 (1985); M. J. Hirsch, U. Thomanschefsky, and D. F. Holcomb, Phys. Rev. B **37**, 8257 (1988); G. A. Thomas *et al.*, Phys. Rev. B **25**, 4288 (1982).
[9] A. G. Zabrodskii and K. Zinoveva, Zh. Eksp. Teor. Fiz. **86**, 727 (1984) [Sov. Phys. JETP **59**, 425 (1984)].
[10] S. Bogdanovich, M. P. Sarachik, and R. N. Bhatt, Phys. Rev. Lett. **82**, 137 (1999).
[11] S. Waffenschmidt, C. Pfleiderer, and H. v. Löhneysen, Phys. Rev. Lett. **83**, 3005 (1999).
[12] K. Slevin and T. Ohtsuki, Phys. Rev. Lett. **82**, 382 (1999).
[13] F. J. Wegner, Z. Phys. B **25**, 327 (1976); H. Shima and T. Nakayama, Phys. Rev. B **60**, 14 066 (1999).
[14] H. Fritzsche and M. Cuevas, Phys. Rev. **119**, 1238 (1960).
[15] P. Mitra *et al.*, Phys. Rev. Lett. **99**, 046804 (2007).
[16] R. Misra *et al.*, Phys. Rev. B **79**, 140408(R) (2009).
[17] B. Coqblin, *Electronic Structures of Rare-Earth Metals and Alloys: The Magnetic Heavy Rare-Earths* (Academic, London, 1977).
[18] P. Wölfle and K. A. Muttalib, in *Perspectives of Mesoscopic Physics*, edited by A. Aharony and O. Entin-Wohlman (World Scientific, Singapore, 2010). Note that a factor of $1/4\pi$ is missing from Eqs. (22.8) and (22.10).
[19] J. O. Dimmock and A. J. Freeman, Phys. Rev. Lett. **13**, 750 (1964).
[20] Y. Liu *et al.*, Phys. Rev. Lett. **67**, 2068 (1991).